

1 FAA Text 2017 R2

10Mar17

2
3
4
5 **REVISION 2**

6
7 **The System Fayalite-Albite-Anorthite and the Syenite Problem**

8
9 **S. A. MORSE^{1*}, J. B. BRADY²**

10
11 ¹Department of Geosciences, University of Massachusetts, Amherst, MA 01003-9297, USA.

12
13 ²Department of Geology, Smith College, Northampton, MA 01063, USA

14
15
16 Intended for American Mineralogist

17
18 10 March 2017

19
20 *Corresponding Author. E-mail tm@geo.umass.edu

23 **ABSTRACT**
24

25 The presence in a magma of fayalite, the iron end-member of the olivine binary series, affects the
26 feldspars at pressure by lowering the temperatures at which they crystallize from the magma.
27 Starting with estimates from published literature it becomes obvious that at pressure, fayalite
28 becomes important because the pressure effects on the melting temperatures are very different:
29 large for albite, and small for anorthite. In this experimental study, a powder of fayalite
30 composition was combined with six finely ground natural feldspars from Ab to An₉₇ to make six
31 bulk compositions. Using graphite crucibles in piston-cylinder apparatus at a pressure of 5 kbar,
32 a cotectic in the ternary system was found to run from 1,141°C at An(Fa) to 1,124°C at Ab(Fa),
33 with fayalite contents from 68 to 17 weight percent, respectively. The results can be used to
34 show that ternary feldspars saturated with fayalite and Fe monoclinic pyroxene will crystallize at
35 a 5-kbar multiphase eutectic 1010°C, 56°C below a calculated azeotropic point on the Ab-Or join.
36 The results are used to compare the end points of two very different layered intrusions,
37 Skaergaard and Kiglapait, and to illuminate the nature and origins of syenite and trachyte, which
38 are leucocratic rocks unsaturated with mafic minerals. Because fayalite-saturated melts are
39 responsive to pressure unequally on the feldspar end members, olivine of intermediate
40 composition will have a damped but potentially significant effect on feldspar fractionation in the
41 lower crust of the Earth, possibly affecting the origin of anorthosite and syenite.

42
43
44 **Keywords:** Fayalite, olivine, feldspar, fractionation, melting experiments, syenite origin
45
46
47
48

49

INTRODUCTION

50

51 This study was undertaken to quantify an early estimate about the low temperature of the
52 fayalite-saturated cotectic in the system Fa-An-Ab. The original estimate of this thermal effect
53 was developed by the senior author in ~1988 from published studies of the systems Fa-An and
54 Fa-Ab. Because the fayalite-saturated composition also occurs in some syenites, we considered
55 that rock type and its genesis to be a logical target for comparison.

56 The fayalite component of olivine in crystallizing melts can have a profound effect on the
57 fractionation of plagioclase at pressure because it affects albite and anorthite very differently.
58 The pressure effect is large for albite and small for anorthite, which makes the plagioclase binary
59 loop and the cotectic curve flatter in temperature (Lindsley, 1968). Because of this behavior, the
60 fractionating power of plagioclase is affected by the presence of fayalite, and in principle by the
61 presence of olivine in general. This contribution was designed to quantify the influence of
62 olivine composition on plagioclase fractionation. This was done by finding the cotectic trace in
63 the system Fa-An-Ab at 5 kbar. The results are applied to natural rocks both known and
64 conjectured.

65

66

METHOD OF WORKING

67

68 The purpose of this exercise was to locate the cotectic in the system Fa-An-Ab at 5 kbar
69 pressure and to determine its temperature profile. The method adopted was to work in piston-
70 cylinder apparatus because of our satisfactory experience with this technology (e.g., Morse et al.,
71 2004). We chose to make up the bulk compositions using a mixture of feldspar end members
72 and natural plagioclase in compositions spaced so that observed melting would bracket
73 equilibrium values for the fayalite-plagioclase cotectic. We chose three hours as a nominal run-
74 time in the expectation that at the high temperatures of these experiments, melting would occur if
75 melt is stable.

76 This work has been done by making up a set of six bulk compositions, holding them, three at
77 a time in graphite, at 5 kbar in a piston-cylinder apparatus at a chosen temperature, quenching
78 them, mounting in epoxy, and interpreting them in reflected light. This procedure suffices to
79 show the existence of melt and crystalline phases (if any). It does not afford the time required
80 for determination of equilibrium crystal compositions, which in our experience requires
81 experimental durations of ~24 hr at 5 kbar in graphite (Morse et al., 2004), nor need it do so to
82 define a cotectic. The criterion of relevance is not reversal but reproducibility.

83 In our experiments, there are examples of glass only (quenched melt) above the liquidus, no

84 glass (below the solidus), glass plus feldspar only (on the plagioclase side of the ternary cotectic
85 composition), glass plus fayalite only (on the olivine side of the ternary cotectic composition),
86 and glass plus fayalite plus plagioclase at co-saturation. In our set of 36 experiments (Table S1¹)
87 24 were deemed successful. There are 10 at three-phase cotectic equilibrium and the rest at zero
88 or one solid phase. Three bulk compositions were found to be sub-solidus, without melt, while
89 other bulk compositions in the same crucible were partly melted. A result having melt plus one
90 crystalline phase represents one leg of a three-phase triangle; melt plus two crystalline phases
91 makes a complete three-phase, invariant triangle. Experimental results at An₁₅ and An₆₆ have
92 been studied with SEM and microprobe to characterize examples of crystal and melt
93 compositions.

94 95 **STARTING MATERIALS AND COMPOSITIONS** 96

97 The starting materials for this experimental endeavor were synthetic fayalite and six natural
98 feldspar compositions described in Table 1. The synthetic fayalite was confirmed pure by X-ray
99 diffraction. Of the feldspars, one was an endmember (Amelia albite, Ab, from the Amelia Court
100 House leucogranite, VA), two were blends of endmembers, and three were natural samples from
101 the Kiglapait layered intrusion (e.g., Morse, 2015b). The endmember An was a natural sample
102 from an amphibolite in the Kiglapait contact zone (KI 2072, An₉₇). Plagioclase compositions
103 were made for An₁₅ and An₃₀ by physically adding powdered sample KI 2072 to Amelia albite
104 as described below. To these feldspars, variable amounts of fayalite were added. The resulting
105 list of intended bulk compositions is given in Table 1.

106 This project was begun by estimating the 1-atm ternary cotectic from the studies of Bowen
107 and Schairer (1936) for the binary Fa-Ab, and Schairer (1942) for the binary Fa-An. The results
108 were interpreted as a straight-line cotectic from Fa₆₄ on the Fa-An sideline to Fa₁₆ on the Fa-Ab
109 sideline. The temperature difference on this cotectic was estimated from the 1-atm temperatures
110 on the sidelines to be 1,110 - 1,050 = 60°C. Adjustments to 5 kbar were made from literature data
111 (e.g., Morse, 1994) assuming pressure corrections of 11.6°C/kbar for Fa-Ab and ~4°C/kbar for Fa-
112 An, yielding an estimate for the Fa-saturated span An to Ab of only 20°C. These preliminary
113 values have been superseded by reference to a corrected value for 1-atm melting of albite at
114 1,100°C (Lange, 2003) and a reconsideration of the pressure effect, discussed below.

¹Deposit item AM-16-00000, Table S1. Deposit items are free to all readers and found on the MSA web site, via the specific issue's Table of Contents (go to <http://www.minsocam.org/MSA/AmMin/TOC/>)

115 Mixtures for the experiments were made by weighing, combining, and grinding the
116 components under acetone in a mullite mortar, typically for ~5 minutes. For each of the starting
117 feldspars, fayalite was added to make a bulk composition bracket over a range of fayalite
118 amounts and a range of temperatures. Electron probe compositions of the starting materials are
119 listed in Table 2. The calculated bulk compositions of all the experiments are listed in Table 3
120 by the name of the plagioclase given in column 4. The initial composition brackets in % Fa were
121 mostly small, e.g., 4% Fa for An₁₅ and An₃₀, but 18% Fa for An₄₈, only one value (60% Fa) for
122 An₆₆, and a bracket of 3% Fa for An₉₇.

123 After grinding, the mixed bulk composition powders were dried overnight at 120°C, placed in
124 small glass vials, and stored in a desiccator.

125

126

EXPERIMENTAL

127

128 Melting experiments were made at 5 kbar pressure in a Rockland Research 19mm piston-
129 cylinder apparatus at the Five College Experimental Petrology Laboratory at Smith College. The
130 ~ 7mg samples were packed, three per run, into 1.5 mm diameter holes drilled to a depth of 2.5
131 mm in an 8 mm long graphite rod. This crucible was covered with a <1-mm graphite lid and
132 placed inside a fired pyrophyllite cup with lid. This in turn was placed within a graphite furnace
133 containing MgO spacers below and above the crucible. The furnace was surrounded by a Pyrex
134 tube, then placed into a salt sleeve with a lead foil sheath, then placed in the tungsten carbide
135 core of the cylinder. It was topped by a brass base plug placed inside a pyrophyllite sleeve. An
136 alumina thermocouple sheath with Type D W-Re thermocouple wires crossed over at the tip was
137 fed through the base plug and upper spacer to rest on the top of the fired pyrophyllite cap.

138 In conventional protocol, samples were pressurized hydraulically to about 120% of the
139 working pressure (because pressure drops with heating) and then heated with a run-up in stages
140 with a programmed controller. The pressure was corrected in the 'hot piston-in' routine near and
141 at the chosen run temperature, which was controlled to ~ 1°C and ± 100 bar, generally for three
142 hours, then quenched to 300°C in 20 seconds by turning off the power to the furnace. The
143 retrieved samples in their graphite cylinder were then embedded in epoxy and held in vacuum
144 overnight. The cured 1-inch disks were ground by hand on silicon carbide sheets until the
145 sample showed. The disk was then polished in a succession of diamond grits to 1-micron in a
146 Struers automatic polisher.

147 The experimental data and visual interpretations are summarized in Supplemental Table S1.
148 Most of the experiments were quenched at three hours. A few early experiments were kept at

149 temperature for 6 to 8.5 hours, but only one composition at 7.7 hr (run 3.3 in Table 2) was used
150 in the final array. Of special note is the observation of small blebs of metallic iron in six
151 experiments, signifying reduction in the graphite capsule. These amounted to less than 1% and
152 were found in only two experiments (6.1 and 6.3) that were listed but not definitive in the final
153 results. Some euhedral plagioclase crystals have swallowtail cores. In Run 8.3, fayalite spinifex
154 clusters were observed amongst big euhedral olivines. In run 9.1 plagioclase rims were seen on
155 olivine. Our experience and that of other workers suggests that graphite-saturated equilibria at
156 pressure tends to maintain the oxygen fugacity to values lower than FMQ; in the present case
157 with these bulk compositions the f_{O_2} is clearly lower than the wüstite-magnetite (WM) buffer.

158 Because of the steep temperature gradients in piston-cylinder apparatus (see Watson et al.,
159 2002), our reported temperatures are believed to be precise only to +/- 5°C.

160

161

TEST OF THE EXPERIMENTAL DESIGN

162

163 Our method of working reflects our experience that melting is rapid in this system at
164 temperatures above 1000°C and that the presence of melt speeds the approach to equilibrium.
165 We tested this approach with more detailed analyses of two samples, as shown in the SEM/BEI
166 images and chemical studies of Figure 1 and Table 4, which will best work in unison. In Fig. 1A
167 of nominal composition An₁₅ we observe a pale gray background of melt accompanied by dark
168 plagioclase in many subhedral forms, and white, more rounded, grains of fayalite. The
169 plagioclase contacts against melt have a characteristic bright BEI outline that arises from the
170 mafic rejected solute pushed away by crystal growth. Careful examination will reveal that
171 several dark crystals in the NW and SE corners have calcic cores that are of a lighter gray
172 intensity.

173 In Fig. 1B of plagioclase composition An₆₆ we find no bright BEI outlines and only anhedral
174 to rarely subhedral plagioclase; the sample is annealed but unmelted.

175 Electron microprobe studies of these two experimental samples are shown in Table 4. It is
176 clear from the analyses that the olivine compositions are essentially the same (columns 1,7 and
177 11), even though they do not meet the test of good stoichiometry. The plagioclase composition
178 in FAA 4.1 is An_{15.7}, near the nominal bulk composition of An₁₅. The normative glass (melt)
179 composition is An_{17.7}. We find that both crystal phases are present, so the bulk composition
180 straddles the cotectic at this temperature. We find that some of the plagioclase is zoned but near
181 the expected composition. At these high temperatures we find that the physical mixture (Table
182 1) of finely ground Ab and An₉₇ has, within three hours, yielded crystals and melts that are, as
183 far as we know, essentially on composition. We conclude that reaction rates are sufficiently fast

184 at the experimental conditions for our experiments to approach equilibrium closely and to
185 constrain the location of the desired cotectic, possibly within the measurement limits of +/- 5°C.
186 The experimental liquid and plagioclase compositions are close and therefore the three-phase
187 triangle for the An₁₅ composition is very narrow.

188 Concerns about the possibility that feldspar might not nucleate can be dispelled by looking
189 at Fig. 1B, where several compositions on and near the cotectic have actually nucleated. It is
190 also our experience that we have never yet encountered failure of feldspar to nucleate at pressure,
191 very likely due to the high surface energy of the finely ground samples.

192

193

194

RESULTS FOR THE COTECTIC LIQUIDUS

195

196 A summary of the pertinent experimental results is shown in Table 5, ordered by the
197 plagioclase composition. Details of this table, ordered by experiment number, are furnished in
198 Supplementary Table S1. Compositional brackets on the cotectic can be inferred from the
199 relative amounts of plagioclase and olivine. From the nominal temperature and the fraction of
200 glass observed optically, the best-fit cotectic temperature is shown in the right-hand column.
201 The results of the 5-kbar, fayalite-saturated melting experiments are shown in the ternary plot of
202 Fig. 2. The six bulk feldspar compositions are pure Ab and the five compositions listed along
203 the Ab-An base line. The ternary cotectic is drawn through the space between nearest olivine
204 and plagioclase saturation pairs. It is straight at higher temperatures above An₁₅, then curved to
205 meet the Fa-Ab cotectic. The amount of fayalite is expressed in weight percent, as measured in
206 the mixtures. The melting points of the three corner compositions are given in degrees C at 5
207 kbar. The entire cotectic range of plagioclase compositions is reached in 17 degrees.

208 Of course, this result is relatively meaningless at the high-temperature end because fayalite
209 is not ordinarily found in An-rich rocks. However, as fractionation proceeds, the relevance of
210 the diagram increases. The pair Fa + Ab is an end member almost never found, and cannot occur
211 in the presence of any CaO-bearing phase (Bowen, 1945); in particular, calcic pyroxene.
212 Instead, crystallization of Fa-saturated liquids more likely involves oligoclase and alkali
213 feldspars.

214 The thermal profile of the cotectic in Fig. 2 is shown in Fig. 3. The steepening of the
215 cotectic temperature toward Fa-Ab is chiefly a reflection of the large effect of pressure on
216 temperature for albite as compared to anorthite. This effect is combined with the systematic
217 increase in feldspar relative to olivine.

218

219

EFFECT OF FAYALITE ON TERNARY FELDSPARS

220

221 **Melting of albite, sanidine, and anorthite**

222 As usual the terminology is simplified by using Ab, Or, and An as the compositional end
223 members, but describing the Or component as sanidine when melting is to be considered.

224 At 1-atm albite melts at 1100°C (Lange, 2003) and the pressure effect in her figure 3, 0 to 10
225 kbar, is given by $T^{\circ}\text{C} = 0.36(P^2) + 18.15(P) + 1,100$, for which $R^2 = 1$. At 5 kbar, then, the
226 melting point is 1,182°C and the mean difference is 16.6°C/kbar.

227 At 1-atm sanidine melts incongruently to leucite + melt but metastably by itself at 1,200°C.
228 Its metastable melting behavior is given by Waldbaum and Thompson (1969) in a curve satisfied
229 by the polynomial $T^{\circ}\text{C} = 0.307(P^2) + 18.61(P) + 1,200$, $R^2 = 1$. The mean pressure effect is
230 17°C/kbar and the 5 kbar melting point is 1,285°C. Note the interesting similarity of the
231 coefficients for Ab and Or and the mean pressure effect.

232 The 1-atm system Ab-Or is an azeotrope with an azeotropic point at $X_{\text{Or}} = 0.331$ (Waldbaum
233 and Thompson, 1969) which the authors chose to take as precisely 1/3, a tradition followed here.
234 The temperature at the minimum was taken by these authors as 1,061°C, here corrected to 1,041°C
235 using the Lange correction for Ab. This step for the binary is warranted by the similarities of the
236 Ab and Or coefficients mentioned above. The 5-kbar azeotropic melting point is 1124°C, and
237 here the stable phase is sanidine, well away from the more K-rich breakdown to Lc + L.

238 The ternary feldspar system is completed by addition of An, which melts at 1,553°C at 1-atm
239 and 1,563°C at 5 kbar (Goldsmith, 1980).

240

241 **Melting of fayalite**

242 The metastable melting of fayalite by itself, bypassing the 1-atm incongruent breakdown to
243 Fe plus liquid, is taken to occur at 1,205°C. A high-pressure Simon equation for the melting
244 curve based on Lindsley (1966) was given by Morse (1994) in Fig. 18.24. This relationship is
245 more conveniently represented using temperature as the dependent variable in the polynomial
246 $T^{\circ}\text{C} = -0.0592(P^2) + 7.788(P) + 1205$, which yields 1,243°C at 5 kbar; again, the value of $R^2 = 1$.

247

248

249

AN APPLICATION OF FAYALITE-SATURATED TERNARY FELDSPAR

250

251 **Fayalite-saturated feldspar at 5 kbar**

252 Albite melts at 1,182°C; the sideline Fa-Ab cotectic is at 1,124°C and the difference is 58°C.
253 The azeotropic point at $X_{Or} = 1/3$ melts at 1,124°C, forming a fortuitous isotherm with Fa-
254 saturated albite. Because of the similar pressure effects on Ab and Or, and for lack of any
255 evidence to the contrary, we assume that the Fa effect is the same at the azeotropic point as at the
256 Ab-Fa sideline, and therefore that a Fa-saturated alkali feldspar would melt at 1,124-58 =
257 1,066°C.

258 A result calculated specifically for the terminal ferrosyenite of the Kiglapait intrusion is
259 shown in Fig. 4. The diagram shows a 5-kbar section from An to the alkali feldspar azeotropic
260 point AP at $X_{Or} = 1/3$ on the binary Ab-Or. The temperatures 1,141 and 1,010°C are
261 experimental from this contribution (Fig. 2) and from Morse and Brady (in review), respectively.
262 The temperature of the AP point, 1,066°C, is described above as calculated from the Ab-Or join
263 and then reduced to account for the fayalite saturation. The thermal minimum is represented as
264 an azeotrope lying at 11% ternary An and therefore projecting from Or to An₁₆ on the Ab-An
265 sideline. The bulk composition at this terminal point includes components and indeed crystals of
266 ferrohedenbergite, a CaAl-bearing pyroxene, that requires the feldspar to be calcic relative to
267 pure Ab (Bowen, 1945).

268 We now have three interesting fayalite-saturated thermal points at 5 kbar: the azeotropic
269 point, the experimental, pyroxene-saturated ternary minimum (Fig. 4) at ~An₁₆ as projected from
270 Or (and so lying on the An₁₁ line), and An. The experimental temperature of the natural ternary
271 feldspar eutectic is 56°C below that of the Ab-Or azeotrope.

272

273

VARIABLE OLIVINE COMPOSITIONS

274

275 A derivative ternary diagram can be constructed to show liquids with variable Mg-Fe olivine
276 compositions with plagioclase, as in Fig. 5. The results are guided in part by the 5-kbar
277 experimental studies of troctolites in the Kiglapait intrusion (Morse et al., 2004). Paths are
278 shown for the approximate trends of the Skaergaard and Kiglapait liquids. The locations of
279 average trachyte (TR) and syenite (SY) are taken from Fig. 5, to be discussed. These locations
280 appear to be anomalous in terms of their high Mg ratio and low An content, and are unlikely to
281 have been produced by any simple trajectory of magmatic fractionation. Decompression (see
282 arrow "-P") would move the field boundaries and the sample compositions somewhat closer to
283 the feldspar join. Note that both these compositions are much richer in total (i.e., ternary)
284 feldspar than in plagioclase alone, shown here. One conclusion from this system is that the
285 effect of Mg on the feldspar-richness of syenites and trachytes is not large.

286

287

THE SYENITE PROBLEM

288

289

290

291

292

293

294

295

Because this contribution is mainly about the terminal crystallization of rocks that can be described as syenites, it is pertinent to expand the discussion to a very old problem of that rock type. A glance at Fig. 6 will quickly show the problem. In this paper and others on the Kiglapait intrusion we tacitly assume that prolonged fractional crystallization leads to rocks called syenite (or ferrosyenite) that are mutually saturated with olivine and calcic pyroxene as well as feldspars, whereas nearly 100 percent of what are called syenites and trachytes in the rest of the world are felsic and far from saturation with mafics.

296

297

298

299

300

301

302

303

There is perhaps a general agreement that syenites are fundamentally rocks of alkali feldspars, a few mafic phases, and no quartz. But the contrast in color index means that when we say “syenite” we may not understand each other. Indeed, the difference between the Gardar rocks and the evolved rocks of layered intrusions is stark. More troublesome yet is the origin of the most abundant syenites: How do they get to be so felsic? In this they become cousins of anorthosite: felsic leftovers of once-cotectic magmas that have left their mafics behind. They have enough traces of mafics to know that there is considerable variety among them, so it isn't just one magma type that generates these separate magmas that intrude overlying crust.

304

305

306

307

308

309

Is there somewhere lurking among our outcrops a mid-crustal mafic residue of parental syenite? If not, can it be in the basal crust or uppermost mantle, undetected?

One word of caution: the Kiglapait troctolitic magma gives a residue of mafic-saturated syenite about the size of a teacup: $\sim 0.15\%$ (i.e. $\sim 5\text{ km}^3$) of the total magma (Morse, 2015b). Real leucosyenites have had a very different history (e.g., an alkalic magma) to make sizeable intrusions (e.g., Upton, 2013).

310

311

312

313

314

FURTHER CONSIDERATION OF THE PRESSURE EFFECT

315

316

317

318

319

It is significant that Fig. 2 presents the effect of fayalite on plagioclase composition at 5 kbar. At atmospheric pressure the estimated difference between the melting temperatures of fayalite-saturated albite and anorthite is $\sim 60^\circ\text{C}$. The pressure effect is about $16.6^\circ\text{C}/\text{kbar}$ for Fa-saturated albite and only 1.6°C for anorthite. At ~ 6.3 kbar, therefore, the fayalite-saturated

320 temperatures are essentially the same for all values of X_{An} . This result requires that the liquidus
321 and solidus are jointly reduced to a straight line, with loop width zero. That is why the above
322 estimates of plausible loop widths are chosen to be small.²

323 At higher pressures, the fayalite-saturated plagioclase loop is reversed! The next question
324 must then be, is this effect anywhere relevant within the Earth? The answer must be, perhaps
325 surprisingly, yes.

326 Fayalite presumably does not occur with calcic plagioclase, but a significant fraction of it
327 does occur in olivine coexisting with plagioclase in troctolites or olivine gabbros. In a sense,
328 then, all natural olivine at pressure must have some partial effect to narrow the effective
329 plagioclase loop and therefore to reduce the effect of plagioclase fractionation. In more evolved
330 bulk compositions the fayalite effect can reduce zoning and thereby supplement adcumulus
331 growth.

332 At depth in the Kiglapait intrusion the presence of olivine must have some small effect on
333 the fractionation of plagioclase in addition to the more important effect of the augite component
334 of the liquid that affects the activity of silica and therefore, preferentially, of albite (Morse,
335 2014). But our consideration must go deeper. At the base of the crust, what does fractionation
336 do to the origin of anorthosite? Or syenite, for that matter. There is a potential here for the
337 generation of plagioclase at nearly constant composition while mafics sink and feldspar becomes
338 concentrated in the lower crust.

339

340

IMPLICATIONS

341

342 The effect of iron-rich olivine to limit the variability of plagioclase composition is shown to
343 be considerable at modest pressure. The usual assumption of a relatively fat Ab-An loop that
344 drives substantial plagioclase fractionation must be modified if Fe-rich olivine is present in the
345 local magmatic system. This effect ramifies to assumptions about plagioclase fractionation
346 efficiency at moderate pressures, including both cumulus feldspar crystals and their interstitial

²We have not attempted to determine tielines or three-phase triangles in this exercise but these can be estimated as follows. For Fo70 olivine and coexisting plagioclase the value of K_D in linear partitioning (Morse et al., 2004) is 0.52, rising with pressure as the loop width diminishes (e.g., Morse, 2015a). The partition coefficient K_D is inversely proportional to loop width (idem) and has the expected value of 1.0 for Fa-An-Ab at 6.3 kbar, shown here. At the experimental pressure used here, 5 kbar, if the value of K_D is 0.8, the mid-range loop width is 5.6% An; if K_D is 0.9, the width is 2.6%. Either value would be time-consuming to determine experimentally.

347 trapped liquids, if any. It applies especially to any modeling of feldspar-rich, olivine-bearing
348 magmatic systems at lower crustal depths, including the possibility that feldspar crystals may
349 grow, accumulate, and fractionate at constant composition. If then separated from their mafic
350 minerals they might ascend to form felsic rocks ranging from anorthosites to syenites.

351

352 **HISTORY OF THIS STUDY** (by Morse)

353

354 I have in my files an entertaining letter from Hatten S. Yoder Jr. dated at the Geophysical
355 Laboratory on January 27, 1989, including a page of 12 ternary diagrams, all with the base at Ab
356 - An, and each with a different apical phase, in order: Diopside, Wollastonite, Enstatite, Spinel,
357 Silica, Nepheline, Leucite, Sanidine, Fayalite, Forsterite, Åkermanite, and Spinel. Cotectics and
358 peritectics where needed are drawn with neat curves from known or inferred sideline
359 temperatures. It is suggested that such drawings would be good lab exercises for students. In
360 particular, this sentence is found at the end of paragraph 1:

361 "Take special note of the one for fayalite - within 58°C you can run from anorthite to albite!"

362 My response on 26 Feb 1989 mentioned re-emergence of his letter from my desk
363 stratigraphy and continued in paragraph three with a discussion of our small differences for Fa-
364 An-Ab, where I got 36.5% An at the sideline compared to his 27%. [cf. 31% An in Fig. 2:
365 together we bracketed it!]. I refer to my drawings "which I happened to have in my file awaiting
366 your beck and call." We agreed that the temperature range was small, but had not yet considered
367 the pressure effect, in which the steep pressure dependence of Ab-melting tends to overtake the
368 lesser pressure effect of An-melting. My response ended with the fervent desire to have
369 somebody study "my favorite system, Fa-An-Ab-Or." The advent of the piston-cylinder
370 apparatus with graphite crucibles finally made this quest feasible.

371

372 **ACKNOWLEDGMENTS**

373

374 We are grateful to Rob Reisener for sharing his synthetic fayalite powder. We thank Mike
375 Jercinovic for making the SEM studies and electron probe analyses with TM. We recognize the
376 helpful review of the original manuscript by James Scoates, an exhaustive and interesting review
377 of the first revision by Don Lindsley, and we acknowledge the reviews of a second reviewer and
378 the Associate Editor. This article is based on research supported by the National Science
379 Foundation under Award No. EAR 0948095.

380

381

382

SUPPLEMENTARY DATA

383

384 [Supplementary data](#) for this paper are available at ----- online. ([Table S1](#))

385

386

REFERENCES

387

388 Bowen, N. L. (1945). Phase equilibria bearing on the origin and differentiation of alkaline rocks.

389 *American Journal of Science* 243A, 75-89.

390 Bowen, N. L., and Schairer, J. F. (1936). The system, albite-fayalite. *Proceedings of the*

391 *National Academy of Sciences* 22, 345-350.

392 Bryan, W. B., Thompson, G. , Frey, F. A. , and Dickey J. S. (1976). Inferred geologic settings

393 and differentiation in basalts from the Deep-Sea Drilling Project. *Journal of Geophysical*

394 *Research* 81(23), 4285-4304.

395 Fuhrman, M. L., Frost, B. R., and Lindsley, D. H. (1988). Crystallization conditions of the

396 Sybille Monzosyenite, Laramie Anorthosite Complex, Wyoming. *Journal of Petrology* 29,

397 699-729.

398 Goldsmith, J. R. (1980). Melting and breakdown reactions of anorthite at high temperatures and

399 pressures. *American Mineralogist* 65, 272-284.

400 Grove, T. L., Kinzler, R. J., and Bryan, W. B. (1992). Fractionation of mid-ocean ridge basalt

401 (MORB). *American Geophysical Union Monograph* (eds. J.P. Morgan, D.K. Blackman,

402 J.M. Sinton), 71, 281-310. (Table 1 #7)

403 Lange, R. A. (2003). The fusion curve of albite revisited and the compressibility of NaAlSi₃O₈

404 liquid with pressure. *American Mineralogist* 88, 109-120.

405 Le Maitre, R. W. (1976). The chemical variability of some common igneous rocks. *Journal of*

406 *Petrology* 17, 589-598 plus 39 figures.

407 Lindsley, D. H. (1966). Pressure-temperature relations in the system FeO-SiO₂. *Carnegie*

408 *Institution of Washington Yearbook* 65, 244-247.

409 Lindsley, D. H. (1968). Melting relations of plagioclase at high pressure. In Isachsen, Y. W.,

410 ed., *Origin of anorthosite and related rocks*, New York State Museum and Science Service

411 *Memoir* 18, 39-46.

412 McBirney, A. R. , and Naslund, H. R. (1990). The differentiation of the Skaergaard intrusion:

413 A discussion of Hunter and Sparks (*Contrib Mineral Petrol* 95:451-461). *Contributions to*

414 *Mineralogy and Petrology* 104, 235-240.

415 Morse, S. A. (1981). Kiglapait geochemistry IV: The major elements. *Geochimica et*

- 416 Cosmochimica Acta 45, 461- 479.
- 417 Morse, S. A. (1994). Basalts and Phase Diagrams. Corrected and reprinted by Krieger,
418 Melbourne, FL, 493 pp.
- 419 Morse, S. A. (2014). Plagioclase fractionation in troctolitic magma. *Journal of Petrology* 55,
420 2403-2418.
- 421 Morse, S. A. (2015a). Linear partitioning in binary solutions: A review with a novel partitioning
422 array. *American Mineralogist* 100: 1021-1032.
- 423 Morse, S. A. (2015b). Kiglapait Intrusion, Labrador. In Charlier et al. (eds), *Layered Intrusions*
424 Springer-Dordrecht, 589-648.
- 425 Morse, S. A. (Sub judice) Kiglapait Mineralogy V: The feldspars. In revision at *American*
426 *Mineralogist*.
- 427 Morse, S. A. , and Brady, J. B. (In revision). Thermal history of the Kiglapait Upper Zone. In
428 revision for *Journal of Petrology*.
- 429 Morse, S. A. & Ross, Malcolm (2004). Kiglapait mineralogy IV: The augite series. *American*
430 *Mineralogist* 89, 1380-1395.
- 431 Morse, S. A., Brady, J. B., and Sporleder, B. A. (2004) Experimental petrology of the Kiglapait
432 intrusion: Cotectic trace for the Lower Zone at 5kb in graphite. *Journal of Petrology* 45,
433 2225-2259.
- 434 Schairer, J. F. (1942). The system CaO-FeO-Al₂O₃-SiO₂. I. Results of quenching experiments
435 on five joins. *American Ceramic Society Journal* 25, 241-274.
- 436 Schairer, J. F., and Yoder, H. S. (1967). The system Albite-Anorthite-Forsterite at 1
437 Atmosphere. *Yearbook Carnegie Institution of Washington* 65, 204-209.
- 438 Upton, B. G. J. (2013) Tectono-magmatic evolution of the younger Gardar southern rift, South
439 Greenland. *Geological Survey of Denmark and Greenland Bulletin* 29, 124 pp.
- 440 Upton, B. G. J., Martin, A. R., and Stephenson, D. (1990). Evolution of the Tugtutôq Central
441 Complex, South Greenland: A high-level, rift-axial, late-Gardar centre. *Journal of*
442 *Volcanology and Geothermal Research* 43, 195-214. (Table 2)
- 443 Wager, L. R., and Brown, G. M. (1967). *Layered igneous rocks*. San Francisco: Freeman
444 (1968, Edinburgh: Oliver & Boyd): 588 pp.
- 445 Waldbaum, D. R., and Thompson, J. B., Jr. (1969). Mixing properties of sanidine crystalline
446 solutions. I. Phase diagrams from equations of state. *American Mineralogist* 54, 1274-1298.
- 447 Watson, E. B., Wark, D. A., Price, J. D., and Van Orman, J. A. (2002). Mapping the thermal
448 structure of solid-media pressure assemblies. *Contributions to Mineralogy & Petrology* 142,
449 640-652.

450 Watt, S. W. (1966). Chemical analyses from the Gardar Igneous Province, South Greenland.
451 Rapport Grønlands Geologiske Undersøgelse 6: 92 pp.

452

453

CAPTIONS

454

455 **Figure 1.** SEM/BEI images of two experimental results, for FAA 4.1 (A) and FAA 11.3 (B).
456 Melt is plentiful in (A) and the subhedral plagioclase grains have bright BEI outlines. Zoning can
457 be seen in both plagioclase and glass. In (B) no melt is present, nor any bright BEI outlines. The
458 measured plagioclase composition (Table 2) is equal to the input bulk composition (Table 1).

459

460 **Figure 2.** The system Fayalite - Plagioclase at 5 kbar. The cotectic boundary between fayalite
461 and plagioclase is located as shown in weight percent fayalite, since these were the quantities
462 weighed in to make the bulk compositions. The endmember components are pure fayalite and
463 natural feldspars. Compositions An₄₈ and An₆₆ are analyzed plagioclase feldspars from the
464 Kiglapait Intrusion, Labrador (Morse, in review). A mixture of the two plagioclase end members
465 An₀ and An₉₇ was used to create the compositions An₁₅ and An₃₀. All starting materials were
466 finely ground crystalline mixtures whose bulk compositions are indicated along the Ab-An
467 sideline. All but one of the experiments were held at temperature and pressure for 3 hours.
468 Those in the plagioclase field were typically poor in crystals and rich in glass, whereas those in
469 the olivine field typically contained tens of percent olivine. The total temperature range from
470 fayalite-saturated pure An to pure Ab is estimated at 17°C.

471

472 **Figure 3.** Temperatures along the cotectic trace of Figure 1. The fayalite contents in Wt. % are
473 given at each determined point. The sample at An₄₈ appears to have an abnormally low
474 temperature and can be raised by 5°C within experimental error.

475

476 **Figure 4.** A calculated 5-kbar *T-X* phase diagram to show the thermal effect of saturating the
477 feldspars with fayalite. The anorthite temperature is taken directly from the ternary diagram
478 (Figure 1) and is not of petrologic interest. The implied azeotropic minimum at 1,010°C is the 5-
479 kbar endpoint of the Kiglapait fractionation history reported in Morse and Brady (in review)
480 representing the terminal reaction liquid = feldspar (cryptoperthite) + olivine + ferrohedenbergite
481 + apatite + ilmenite. The temperature plotted at Ab is that of the fayalite - saturated binary
482 minimum at $X_{Or} = 1/3$ on the Ab-Or sideline, calculated as described in the text. The final liquid
483 owes its An-rich composition to the presence of the Ca-Al-Fe pyroxene known from experiment

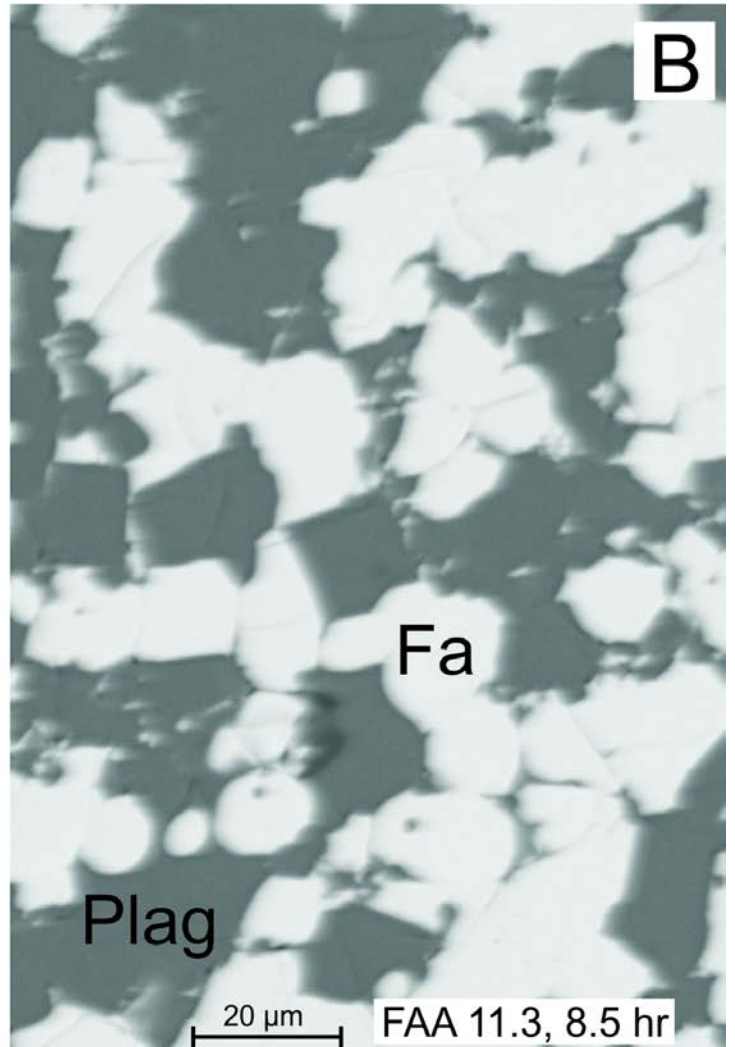
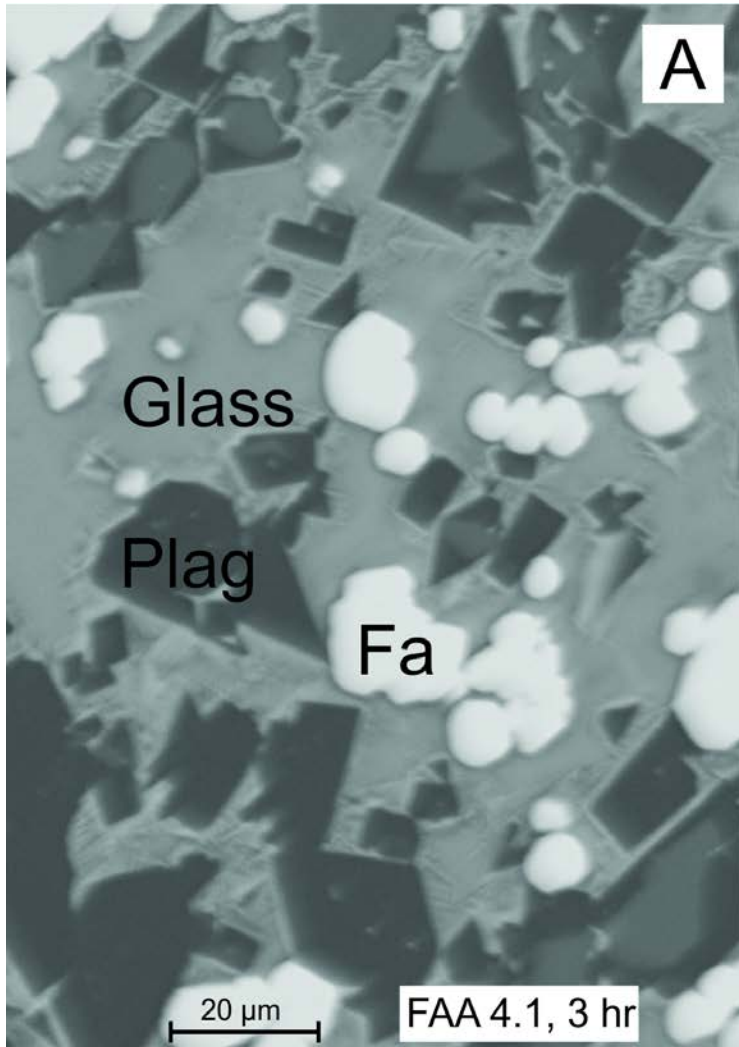
484 to have lost Al to feldspar during cooling (Morse and Ross, 2004). The temperature drop of 56 °C
485 recalls Bowen's (1945) "plagioclase effect" in which it is understood that no pure albite can
486 crystallize from a magma containing Ca. Abbreviation: Ap, Azeotropic point.

487

488 **Figure 5.** The system Olivine - Plagioclase at 5 kbar, in oxygen units, contoured in X_{Mg} . The
489 heavy line nearest the OL corner is the cotectic for the system Fa-Ab-An, converted from Figure
490 2. The lowermost cotectic line is that for the system Fo-An-Ab (Schairer & Yoder, 1967),
491 recalculated to 5 kb, and the intervening lines of variable X_{Mg} are interpolated. The arrows
492 shown for the Kiglapait (KI) and Skaergaard (SKD) Intrusions are net LIQUIDUS paths between
493 the endpoints, taken from Morse et al. (2004) and Morse (1981) in the first case, and from
494 McBirney & Naslund (1990) and Wager & Brown (1968) in the second case. The fractionation
495 paths of the layered intrusions are taken as guides to magma evolution in general in this
496 composition space. The notation "-P" with arrow signifies decompression. The vertical line at
497 An_{50} is simply a guide to the eye.

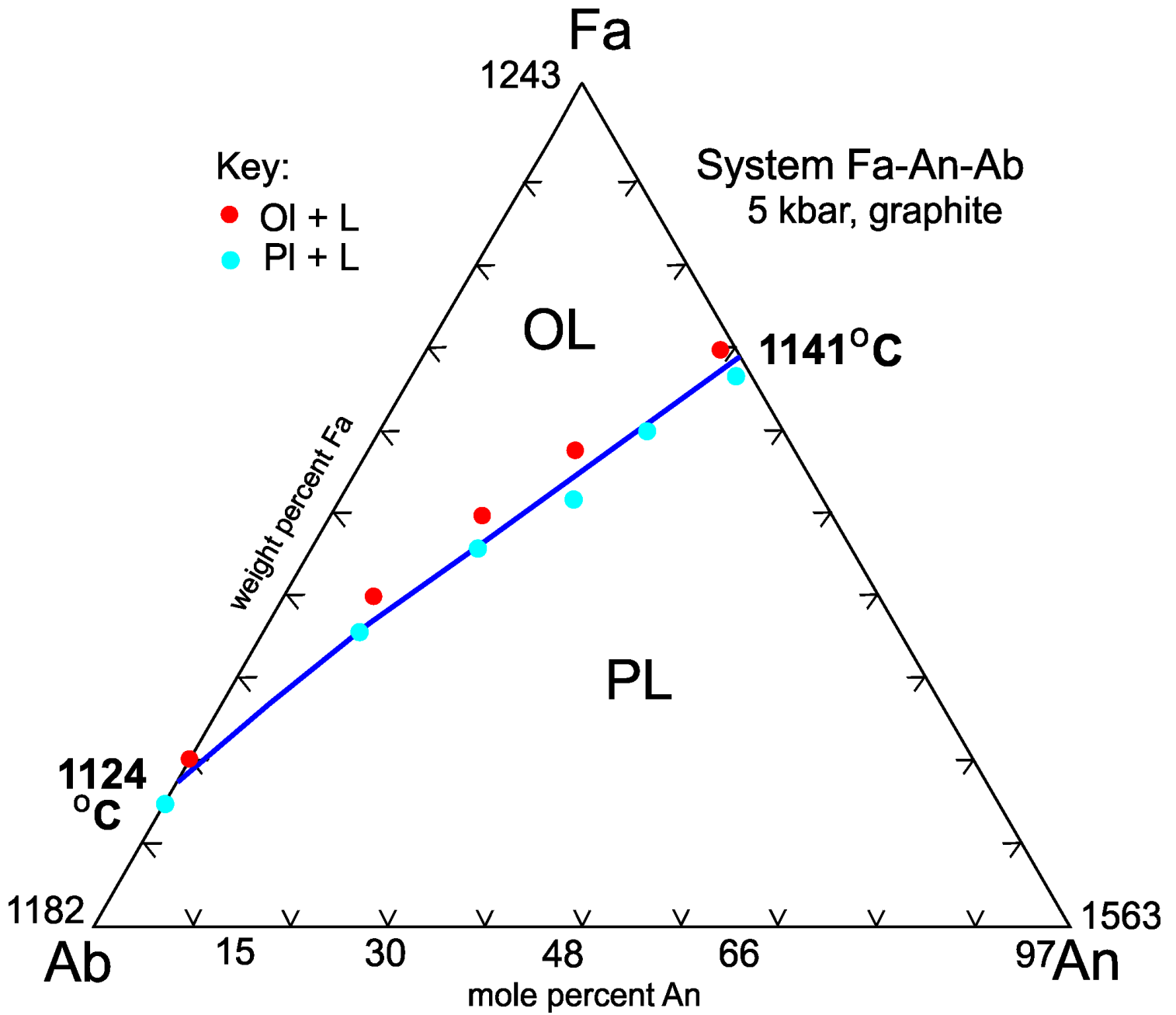
498

499 **Figure 6.** (A) Ternary plot of olivine + hypersthene (OLHY), feldspar (FSP), and augite (AUG)
500 referred to a weight ferrous ratio $FeO/(FeO+Fe_2O_3) = 0.9$. The solid line is the experimental
501 cotectic trace of liquid + Ol + Pl for the Lower Zone of the Kiglapait intrusion (Morse et al.,
502 2004), from an initial composition at 5.2% AUG to saturation with augite at 24.5% AUG. The
503 cross marked IBZ is the average of three rock compositions from the Kiglapait Inner Border
504 Zone. The solid circles (KI SY) are the compositions of the six uppermost syenites in the
505 intrusion (Morse, 1981); the red dot is the average of the two uppermost samples. MORB
506 compositions are plotted to illustrate their near-saturation with augite; the upper symbol is a glass
507 from Grove et al. (1992); the lower symbol is the average of 155 Atlantic glasses from Bryan et
508 al. (1976). Compositions of average syenite and trachyte are from Le Maitre (1976). The
509 Gardar SY is an average of 8 Kûngnât syenites from Watt (1966). The symbol SYB refers to the
510 Sybille monzosyenite, Wyoming, from Table 2 of Fuhrman et al. (1988). The arrow labeled
511 MELTS shows the calculated result of feldspar fractionation from a saddle syenite composition
512 in Tugtutôq Central Complex of South Greenland (Upton et al. 1990, Table 2). The end of the
513 arrowhead denotes the premature appearance of olivine in the calculation. (B) Compositions of
514 syenite and trachyte in terms of feldspar end members An and Or, plotted against Mg number;
515 abbreviations as in (A).



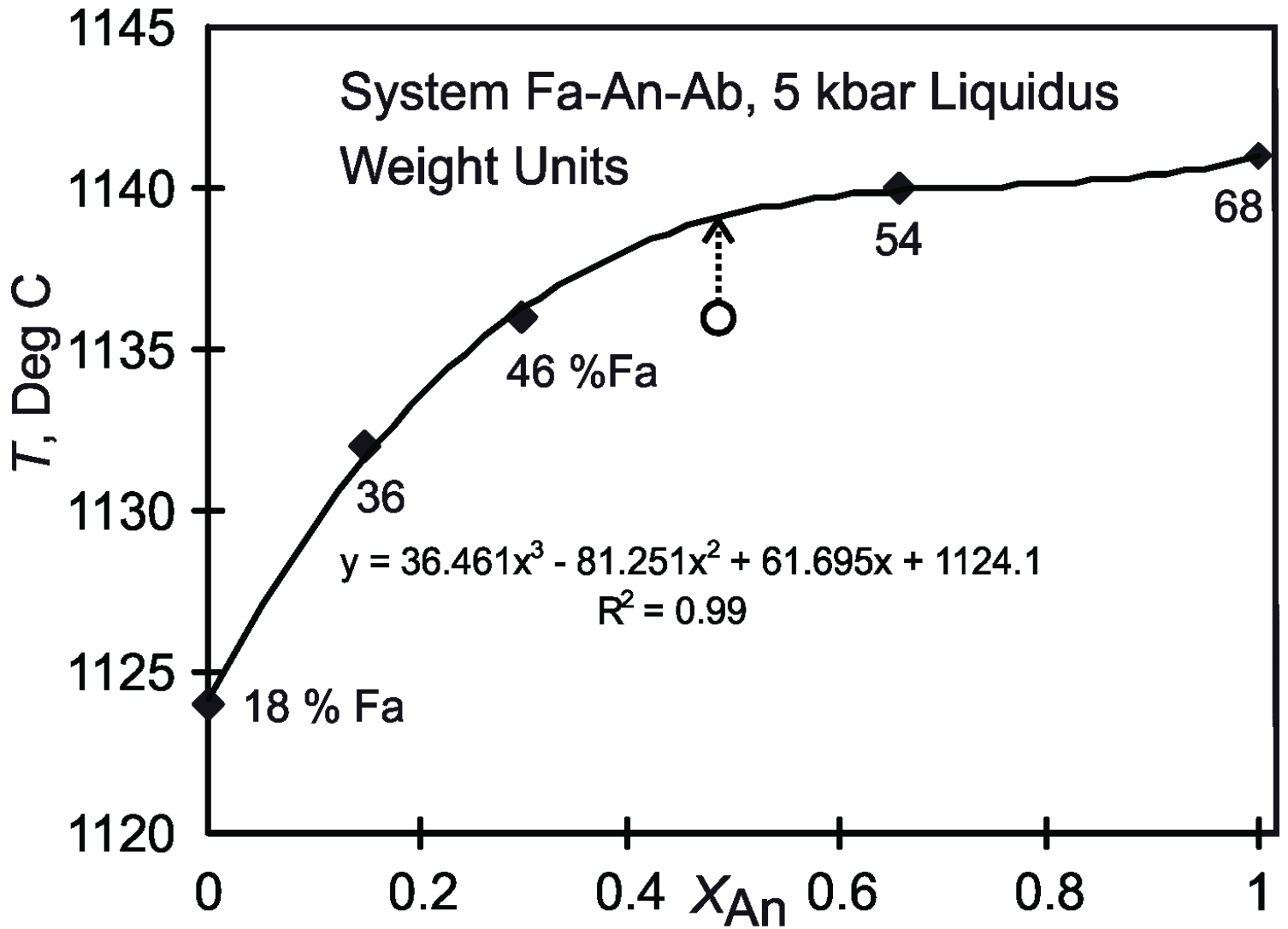
FAA SEM 1

Morse-Brady Fig. 1



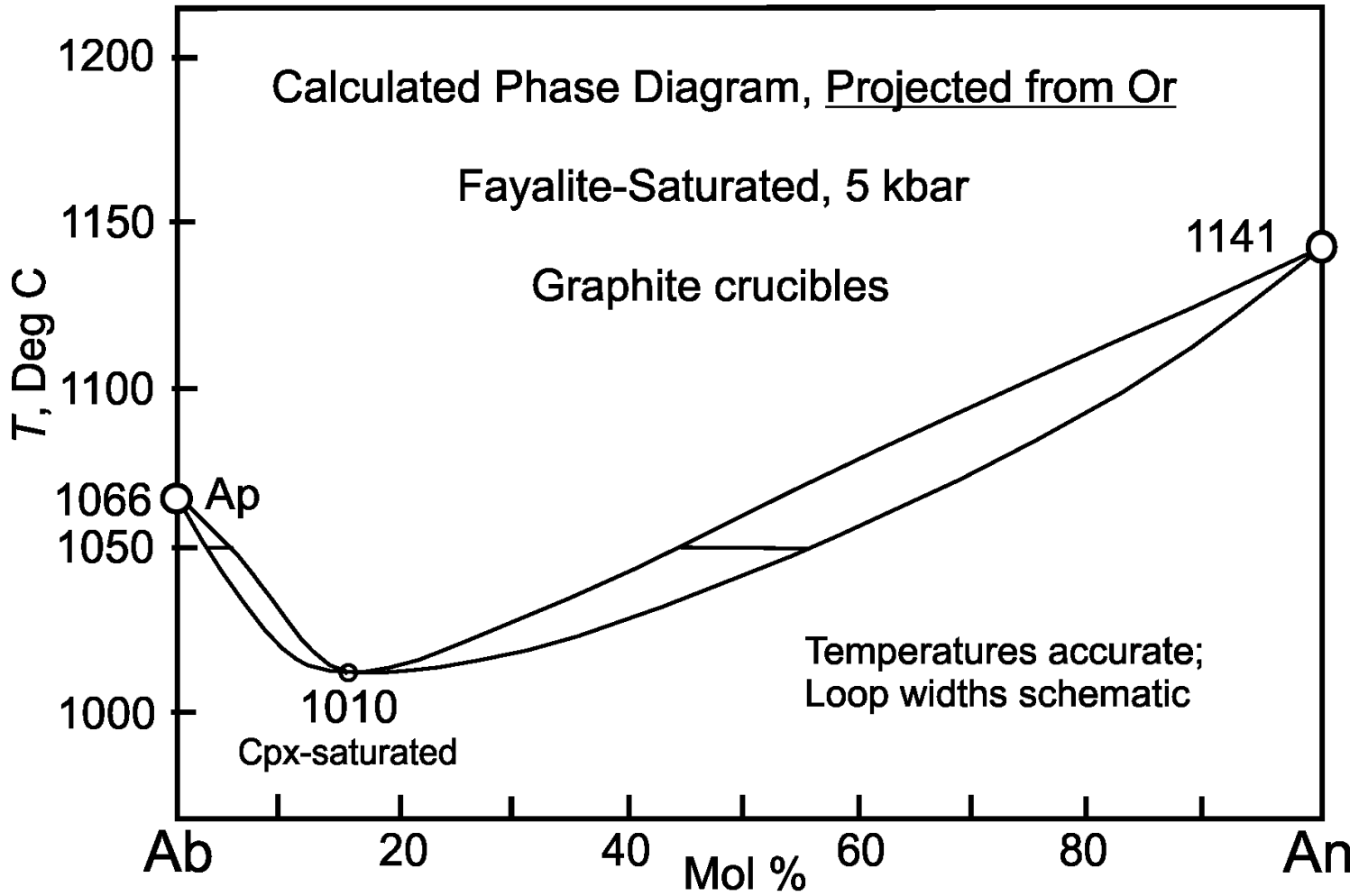
FAA Tern 16
9 Feb 16

Morse-Brady Fig. 2
"Color online"



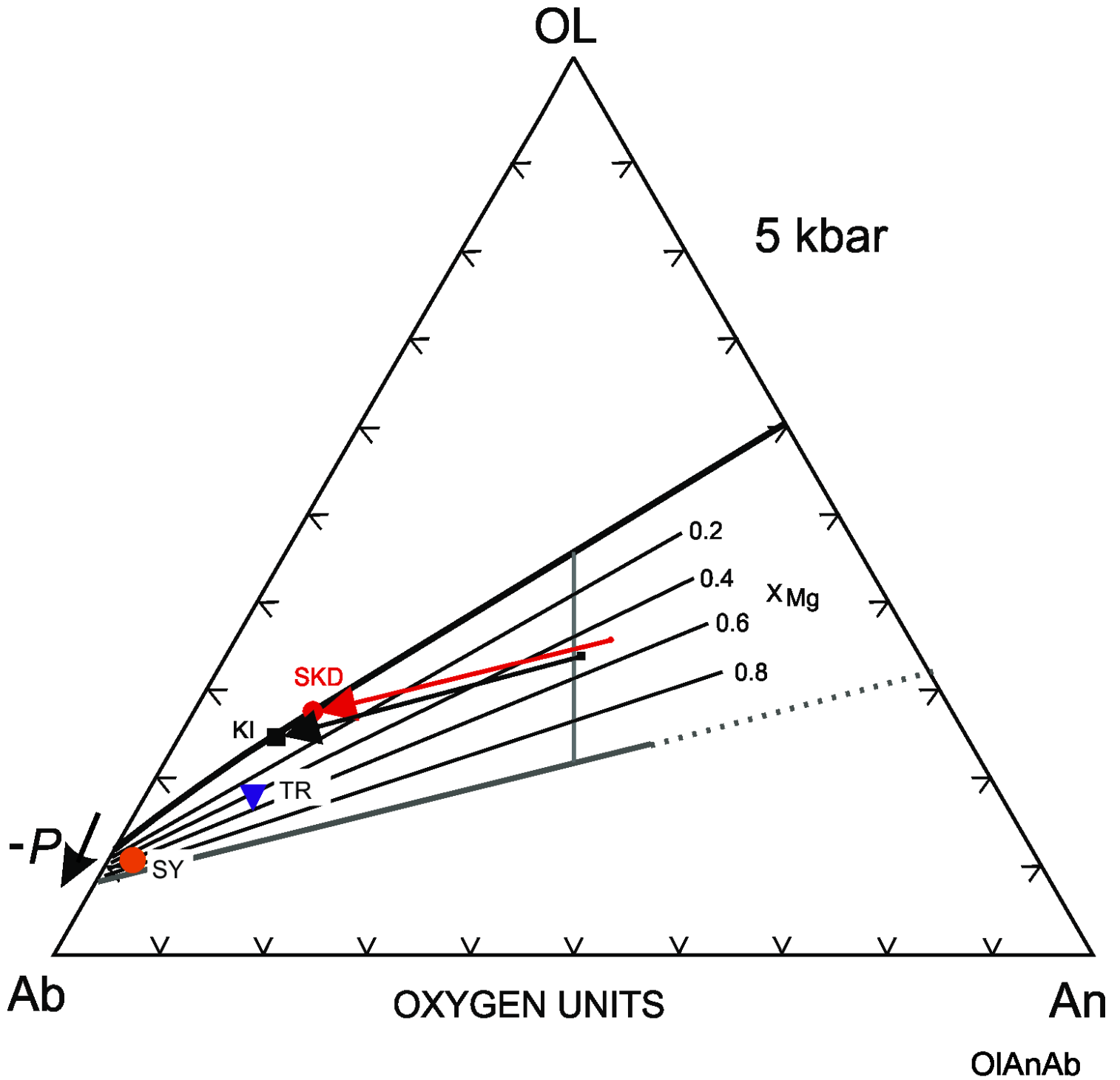
FaAnAb 09 15

Morse-Brady Fig. 3

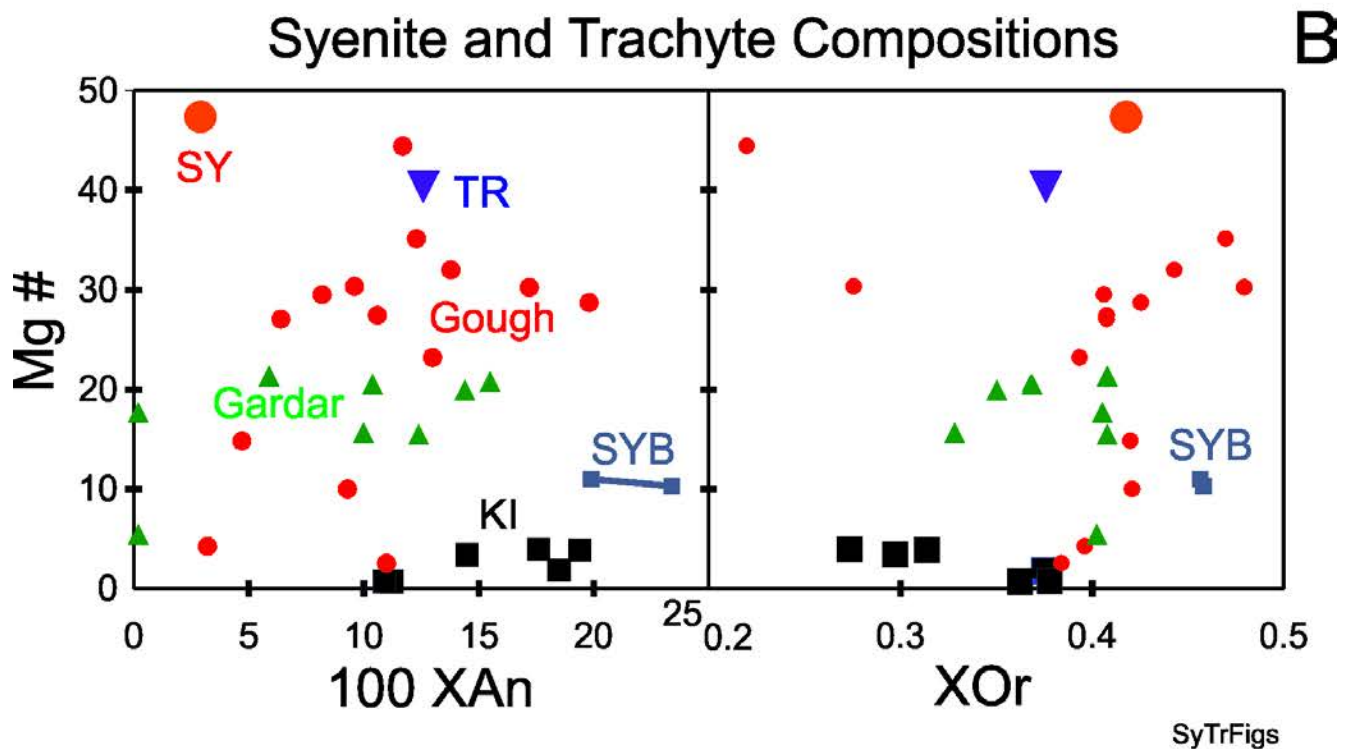
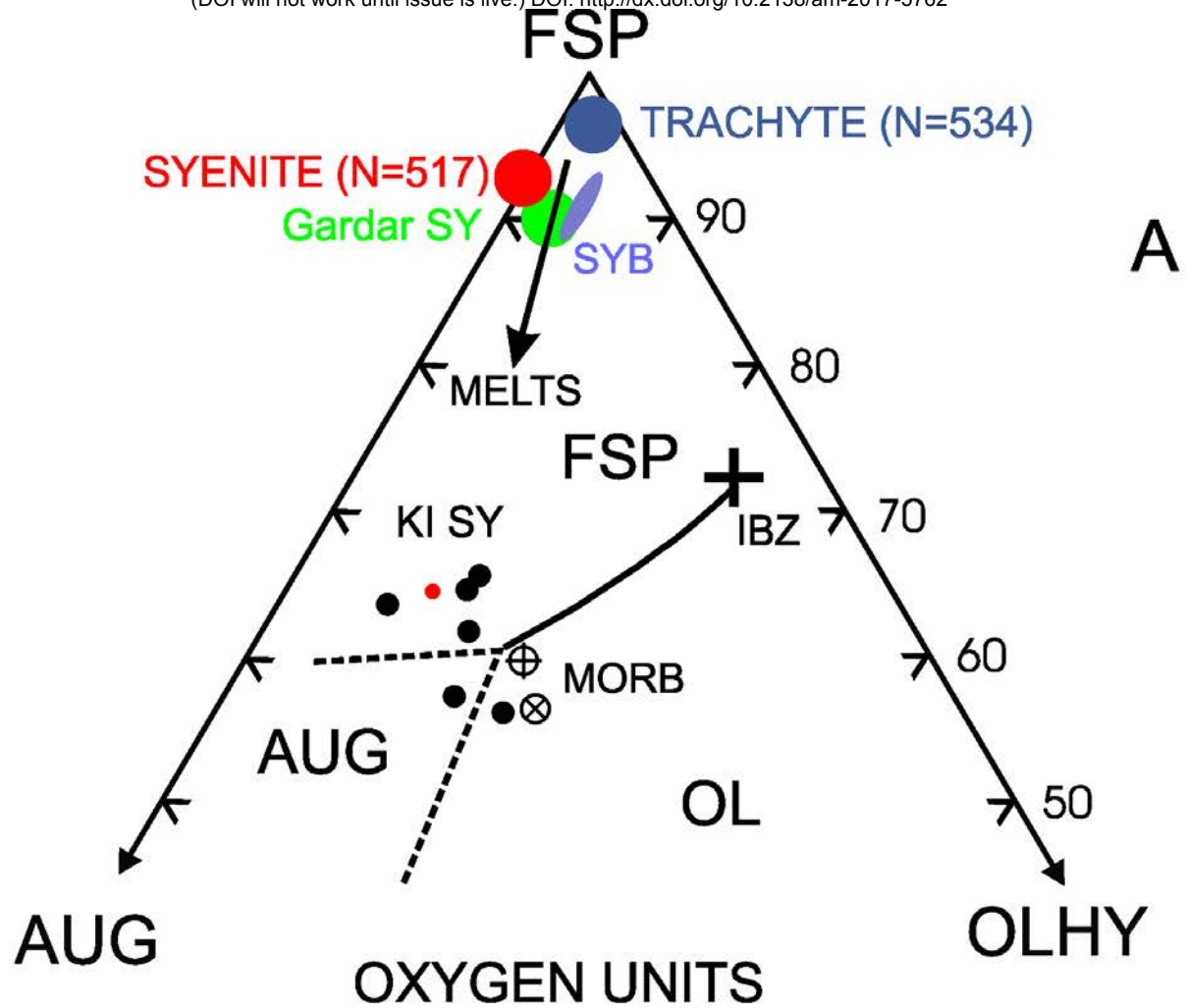


Conc Ph Diag 3
9 Feb 16

Morse-Brady Fig. 4



Morse-Brady Fig. 5
"Color online"



Morse-Brady Fig. 6
 "color online"

Table 1. System Fa-An-Ab						
Measured starting compositions, from oxygen norms.						
Starting Material:						
	Amelia	An+Ab	An+Ab	KI 3369	KI 3645	KI 2072
Composition Target	An 0	An 15	An 30	An 48	An 66	An 97
Expected An	0.47	15	30	48.3	66.1	97
Probe result	0.47	14.8	30	48.5	66.2	97
	Crystal	Glass	Glass	Crystal	Crystal	Crystal

Table 2. Electron microprobe compositions of starting materials							
(Normalized to 100)							
Sample:	Fayalite	Amelia	An 15*	An 30*	An 48.3	An 66.1	KI 2072
SiO ₂	29.48	68.24	64.27	60.26	56.04	41.51	41.1
TiO ₂	0	0	0	0	0.08	0.08	0
Al ₂ O ₃	0	19.48	22.03	24.8	27.86	30.71	37.1
Fe ₂ O ₃	0	0	0	0	0.09	0.25	0
FeO	70.52	0	0.05	0.09	0.25	0.15	0.28
MgO	0	0	0	0	0.06	0.14	0
CaO	0	0.10	3.25	6.44	9.6	13.21	21.3
Na ₂ O	0	12.03	10.17	8.3	5.67	3.74	0.35
K ₂ O	0	0.15	0.13	0.1	0.34	0.21	0
Total	100	100	100	100	100	100	100
An, Mol %	0	0.5	15	30	48.3	66.1	97.0
Samples with * are mixtures of Amelia albite and An 97							

Table 3. Bulk Compositions of experiments

BC #	% Fa	% Plag	Plag Name	XAn	Ternary		
					An	Ab	Or
Amelia		100	Am	0.005	0.0047	0.9872	0.0081
KI 3369pl		100	An48	0.483	0.474	0.506	0.020
KI 3645pl		100	An66	0.661	0.653	0.335	0.012
KI 2072pl		100	An97	0.970	0.970	0.030	0
An15		100	An15	0.146	0.146	0.854	0.007
An30		100	An30	0.291	0.291	0.709	0.006
BC1	15	85	Am	0.005	0.004	0.846	not calc
BC2	25	75	Am	0.005	0.004	0.746	--do--
BC3	40	60	An48	0.483	0.290	0.310	--etc--
BC3a	36	64	Am	0.005	0.003	0.637	
BC3b	55	45	An48	0.483	0.217	0.233	
BC4	36	64	An15	0.015	0.010	0.630	
BC4a	36	64	An15	0.015	0.010	0.630	
BC5	46	54	An30	0.03	0.016	0.524	
BC5a	46	54	An30	0.03	0.016	0.524	
BC6	58	42	An48	0.483	0.203	0.217	
BC7	60	40	An66	0.661	0.264	0.136	
BC8	67	33	An97	0.97	0.320	0.010	
BC9	70	30	An97	0.97	0.291	0.009	
BC10	40	60	An15	0.146	0.088	0.512	
BC11	50	50	An30	0.291	0.146	0.355	
BC12	20	80	Am	0.005	0.004	0.796	
BC13	53	47	An48	0.483	0.227	0.243	
BC14	17	83	Am	0.005	0.004	0.826	
BC15	10	90	Am	0.005	0.005	0.896	

Experiments An 15, 2; An30, 2; An 48, 4; An 66, 1; An 97, 2

Table 4: Two electron probe results in the system Fa-An-Ab

	Exper # FAA 4.1						Exper # FAA 11.3				
	OLIVINE	SD	PLAGIO- CLASE	SD	GLASS	SD	OLIVINE	SD	PLAGIO- CLASE	SD	OL(4) - OL(11)
SiO2	31.03	0.41	63.34	0.36	52.31	0.26	30.94	0.30	50.01	1.10	0.09
TiO2	0.01	0.01	0	0	0.00	0.00	0.00	0.00	0.03	0.02	0.01
Al2O3	0.12	0.20	22.42	0.49	14.70	0.34	0.12	0.13	30.76	0.91	0.00
FeO	68.52	0.58	1.57	0.84	25.53	0.66	68.40	0.64	1.70	0.86	0.12
MgO	0.13	0.02	nd		0.02	0.01	0.13	0.01	nd		0.00
CaO	0.20	0.05	3.31	0.34	2.12	0.33	0.40	0.04	13.54	0.94	-0.20
Na2O	nd		9.81	0.13	5.36	0.33	nd		3.81	0.49	
K2O	nd		0.05	0.01	0.03	0.01	nd		0.15	0.04	
Sum	100.00*	0.37	100.5		100.20		100.00**		100.00***		
N	12		8		12		12		12		
					P2O5 0.04						
	Fo 0.03		An 15.7		An 17.7				An 66.2		

(*) normalized from 101.00
 (**) normalized from 100.89
 (***) normalized from 99.13
 Note: Mn in olivine = 0.00

Table 5. System Fayalite-Albite-Anorthite, 5 kbar

Comp	% Fa	Run	T deg C	% OL	% PL	% Glass	Interpreted Result
An 0	15	1.1	1120	0	10	90	
	25	2.1	1125	0	1	99	LIQUIDUS 1124
	25	9.1	1125	25	1	74	
An 15	20	10.1	1125	25	10	65	
	36	4.1	1120	30	20	50	LIQUIDUS 1132
	36	6.1	1130	2	0	98	
An 30	36	10.2	1125	40	10	65	
	40	9.2	1125	40	0	60	
	46	4.2	1120	35	25	40	LIQUIDUS 1134
An 30	46	7.1	1135	0	0	100	
	50	9.3	1125	50	0	50	
	46	10.3	1125	45	25	30	
An 48	46	11.1	1128	45	10	45 T?	
	46	12.2	1133	40	30	30	
	40	1.3	1120	0	50	50	LIQUIDUS 1136?
An 48	40	3.3	1122	0	40	60	
	58	6.3	1130	1	0	98	
	58	7.2	1135	0	0	100	
An66	53	11.2	1128	60	40	0	
	53	12.3	1133	50	50	0	
	60	8.1	1140	0	0	100	LIQUIDUS 1138?
An66	60	11.3	1128	70	30	0	
	An 97	67	8.2	1140	0	4	96 T>1140
An 97	70	8.3	1140	30	5	45	